

Crack-tip constraint analysis of two collinear cracks under creep condition

Guang-Chen Jiao^{1a}, Wei-Zhe Wang^{*1,2} and Pu-Ning Jiang^{1b}

¹Key Lab of Education Ministry of China for Power Machinery and Engineering, Shanghai Jiao Tong University, Shanghai 200240, P.R. China

²Stat Key Laboratory of Mechanical System and Vibration, Shanghai Jiao Tong University, Shanghai 200240, P.R. China

(Received December 4, 2011, Revised March 27, 2012, Accepted June 1, 2012)

Abstract. The higher-order asymptotic $C(t) - A_2(t)$ approach was employed to investigate the crack-tip stress of two collinear cracks in a power-law creeping material under the plane strain conditions. A comprehensive calculation was made of the single crack, collinear crack model with $S/a = 0.4$ and 0.8 , by using the $C(t) - A_2(t)$ approach, HRR-type field and the finite element analysis; the latter two methods were used to check the constraint significance and the calculation accuracy of the $C(t) - A_2(t)$ approach, respectively. With increasing the creep time, the constraint A_2 was exponentially increased in the small-scale creep stage, while no discernible dependency of the constraint A_2 on the creep time was found at the extensive creep state. In addition, the creep time and the mechanical loads have no distinct influence on accuracy of the results obtained from the higher-order asymptotic $C(t) - A_2(t)$ approach. In comparison with the HRR-type field, the higher-order asymptotic $C(t) - A_2(t)$ solution matches well with the finite element results for the collinear crack model.

Keywords: constraint; creep; plane strain; interacting cracks; $C(t) - A_2(t)$ approach

1. Introduction

Multiple cracks associated with corrosion and welding flaws frequently occur in high temperature components of aerospace structures, pressure vessels and nuclear reactors. In practical condition, the presence of multiple cracks may seriously degrade damage tolerance of structures. The stress state at the crack-tip field would be abruptly intensified due to strong interaction of the closely spaced multiple cracks, resulting in the accelerated crack growth. Accordingly, rapid prediction of the stress and deformation state at the crack-tip field of the interacting multiple cracks is of considerable significance to structure integrity evaluation of high temperature components (Liu *et al.* 2008).

Numerous numerical efforts have sought to understand the influence of the interacting multiple cracks on the crack-tip stress field. By using the finite element method, Si *et al.* (2008) performed creep analysis of two interacting semi-elliptical cracks, yielding an empirical rule of evaluating the

*Corresponding author, Associate Professor, E-mail: wangwz0214@sjtu.edu.cn

^aPh.D. Candidate, E-mail: jgc_101983@163.com

^bResearch Scholar, E-mail: jiangpuning@yahoo.com.cn

interacting cracks. Chen *et al.* (2009) evaluated T-stress of the interacting cracks by using complex variable function method. Kamaya (2008) employed finite element analysis to determine the growth of the interacting multiple surface cracks by calculating the stress intensity factor. Xuan *et al.* (2009) developed a closed form solution to evaluate the interaction of two cracks in plates under tension. In addition, some fitness of service codes were developed for safety assessment, e.g., ASME Boiler and Pressure Vessel Code Section XI (2004), API579 (2007), BS7910 (2005) and R6 (2006).

The crack-tip stress and strain rate fields under the creep condition are normally determined as the function of the time-dependent contour integral $C(t)$. At the steady state or under extensive creep condition, the time-independent contour integral C^* is used for the value of $C(t)$ (Kim *et al.* 2002, Assire *et al.* 2001, Fookes and Smith 2003). However, the dominant zone of the HRR-type method based on the $C(t)$ -integral theory is highly limited in the spatial scale, which is attributed to the fact that the stress constraint under the plane strain condition was not taken into account (Yang *et al.* 1996). This means that careful consideration of the crack-tip constraint is needed in a view to enlarge the dominant zone. Toward this end, a few two-parameter approaches on the basis of elastic-plastic mechanics were proposed to rapidly evaluate the constraint effect on the crack-tip field, e.g., J - T approach (Betegon and Hancock 1991), J - Q approach (O'Dowd *et al.* 1991) and J - A_2 approach (Yang *et al.* 1993, Chao and Zhu 1998); these approaches are mainly developed for the situations at room temperature. As for the creeping materials at the elevated temperature, the $C(t)$ - $Q(t)$ (Shih *et al.* 1993, Sharma *et al.* 1995) and $C(t) - A_2(t)$ (Chao *et al.* 2001, Hutchinson 1968) approaches were mainly developed to evaluate the constraint effect on the crack-tip field. However, the $C(t) - Q(t)$ approach (Shih *et al.* 1993) was derived from the J - Q approach, which is unfortunately only applicable under small-scale yielding condition in comparison to the J - A_2 approach. Subsequently, Chao *et al.* (2001) extended the J - A_2 approach for the elastic-plastic materials to the higher-order asymptotic $C(t) - A_2(t)$ approach for the creeping materials. A comparative study of the crack-tip constraint of the single edge notched tension specimen demonstrated that the dominant zone of the $C(t) - A_2(t)$ approach is obviously larger than that of the approach based on HRR solution (Chao *et al.* 2001). In recent years, the constraint parameter Q and a new constraint parameter R (Wang *et al.* 2010, 2012, Sun *et al.* 2011) are used to study the constraint at the crack tip for different cracked models, such as compact tension (CT) specimen, middle-cracked tension (MT) specimen, single edge-notched bend (SENB) specimen and single edge-notched tension (SENT) specimen. For the aspect of the research on crack growth rate, some experimental and theoretical evidences have shown that constraint can also affect creep crack growth rate under creep conditions (Budden and Dean 2007). For the 316H austenitic steel, the deviation of the crack growth rate between the middle-cracked tension (MT) specimen and the compact tension (CT) specimen (Bettinson *et al.* 2002) have been found. However, few literature survey on the constraint analysis at the crack tip by using the higher-order asymptotic $C(t) - A_2(t)$ approach was found. Accordingly, investigation of the constraint parameter at the crack tip by using the higher-order asymptotic $C(t) - A_2(t)$ approach is highly desirable.

In the present study, the higher-order asymptotic $C(t) - A_2(t)$ approach was employed to rapidly predict the crack-tip stress fields of two collinear cracks at the elevated temperature. The material investigated in the present paper is Cr-Mo rotor steel. The influence of the material hardening exponent n , horizontal distance between two cracks, and mechanical load on the crack-tip constraint A_2 was evaluated. The results demonstrated that the higher-order asymptotic $C(t) - A_2(t)$ solution matches well with the finite element analysis, whereas a large deviation was found for the calculations by using the HRR-type field.

2. Mathematical method

In calculation, the main attention was directed to the two-dimensional stationary crack problem under the plane strain condition. In the present study, the higher-order asymptotic $C(t) - A_2(t)$ approach was employed to investigate the influence of material hardening exponent, horizontal distance between two cracks, and mechanical load on the constraint at the crack-tip field. The calculations by using the HRR-type approach and finite element method were provided for comparison. Hereafter, the mathematical fundamentals of the higher-order asymptotic $C(t) - A_2(t)$ approach are briefly introduced.

In the current study, mechanical properties of low alloy Cr-Mo steel are used. The deformational behavior of the material under the plane strain condition is governed by the elastic-nonlinear viscous constitutive relation. Under the uni-axial tension, the total strain rate is related to stress in terms of the Norton power-law creep relation

$$\dot{\varepsilon} = \frac{\dot{\sigma}}{E} + \dot{\varepsilon}_0 \left(\frac{\sigma}{\sigma_0} \right)^n \quad (1)$$

where $\dot{\varepsilon}$ is the uni-axial strain rate, $\dot{\sigma}$ is the uni-axial stress rate, E is Young's modulus, n is the creep exponent, σ_0 is the yield stress, and $\dot{\varepsilon}_0$ is the creep strain rate. Note that the combined creep coefficient $B = \dot{\varepsilon}_0 / \sigma_0^n$ is often used. The material properties (Si *et al.* 2008) were listed in Table 1.

To describe the strain rate of the material under the multi-axial stress state, the uniaxial creep relation is rewritten as

$$\dot{\varepsilon}_{ij} = \frac{1+\nu}{E} \dot{S}_{ij} + \frac{1-2\nu}{3E} \sigma_{kk} \delta_{ij} + \frac{3}{2} \dot{\varepsilon}_0 \left(\frac{\sigma_e}{\sigma_0} \right) \frac{S_{ij}}{\sigma_0} \quad (2)$$

where ν is the Poisson ratio, δ_{ij} is the Kronecker delta, $\dot{\varepsilon}_{ij}$ is the strain rate tensor, σ_{ij} is the stress tensor, S_{ij} is the deviatoric tensor of stress ($S_{ij} = \sigma_{ij} - \sigma_{kk} \delta_{ij} / 3$), and σ_e is the Mises effective stress.

To describe the stress and strain states at the crack-tip field, the HRR-type singularity field (Hutchinson 1968, Rice and Rosengren 1968) for the power-law creep material is determined to

$$\sigma_{ij} = \sigma_0 \left(\frac{C(t)}{\dot{\varepsilon}_0 \cdot \sigma_0 \cdot I_n \cdot r} \right)^{1/n+1} \cdot \tilde{\sigma}_{ij}(\theta) \quad (3)$$

where r and θ are the polar coordinates. In Eq. (3), the dimensionless constant I_n and normalized function $\tilde{\sigma}_{ij}$ are functions of the creep exponent n . The time-dependent contour integral $C(t)$ (Bassani and McClintock 1981) is defined as

$$C(t) = \int_{\Gamma} \left(\dot{W} dy - \sigma_{ij} n_j \frac{\partial \dot{u}_i}{\partial x} d\Gamma \right) \quad (4)$$

in which the notation Γ is the integral path enclosing the crack tip, n_j is the unit outward vector, \dot{u}_i is the displacement rate vector, and the strain energy rate density is $\dot{W} = \int_0^{\dot{\varepsilon}_{ij}} \sigma_{ij} d\dot{\varepsilon}_{ij}$.

As mentioned earlier, the dominant zone of the HRR-type singularity field is highly limited in the

Table 1 Material constants used in analysis

E (MPa)	ν	B (MPa ⁻ⁿ /h)	n
200000	0.3	5.0E-12	3

spatial scale. To increase the dominant zone, the higher-order asymptotic solution, which characterizes the stress field near the crack tip in the creeping material (Chao *et al.* 2001), is given by

$$\frac{\sigma_{ij}(r, \theta, t)}{\sigma_0} = A_0(t)[r^{s_1} \cdot \sigma_{ij}^{(1)}(\theta) + A_2(t) \cdot r^{s_2} \cdot \sigma_{ij}^{(2)}(\theta) + A_2^2(t) \cdot r^{s_3} \cdot \sigma_{ij}^{(3)}(\theta)] \quad (5)$$

where, $A_0(t) = \left(\frac{C(t)}{\sigma_0 \dot{\epsilon}_0 I_n L}\right)^{1/(1+n)}$ and $s_1 = -\frac{1}{n+1}$.

At the steady state or under extensive creep condition, the time-dependent contour integral $C(t)$ and the constraint parameter $A_2(t)$ approach to the time independent contour integral C^* and A_2^* , respectively. Hence, the higher-order asymptotic solution is reduced to

$$\sigma_{ij}(r, \theta) = A_1(t)[r^{s_1} \cdot \sigma_{ij}^{(1)}(\theta) + A_2^*(t) \cdot r^{s_2} \cdot \sigma_{ij}^{(2)}(\theta) + A_2^{*2}(t) \cdot r^{s_3} \cdot \sigma_{ij}^{(3)}(\theta)] \quad (6)$$

where, $A_1(t) = \left(\frac{C^*}{BI_n L}\right)^{1/(1+n)}$.

3. Finite element model

The geometry and the finite element model of the two collinear cracks are shown in Fig. 1. The length of the crack is $2a = 5$ mm, for the two collinear crack model, the horizontal distances between the two cracks are $S = 0.4 * 2a$ and $0.8 * 2a$, respectively. Dimensions of the planar material in length and width are large enough to avoid the boundary effect of the model. For all cases, 20 contours were modeled for calculating the $C(t)$ -integral at the crack-tip field.

For comparison, the finite element analysis of the small-scale and extensive creep was carried out by using ABAQUS. The eight-node isoparametric element with reduced integration (CPE8R in ABAQUS) were introduced to avoid the problems associated with incompressibility; a total of 4288 elements and 13116 nodes were constructed in the finite element analysis. To enhance the

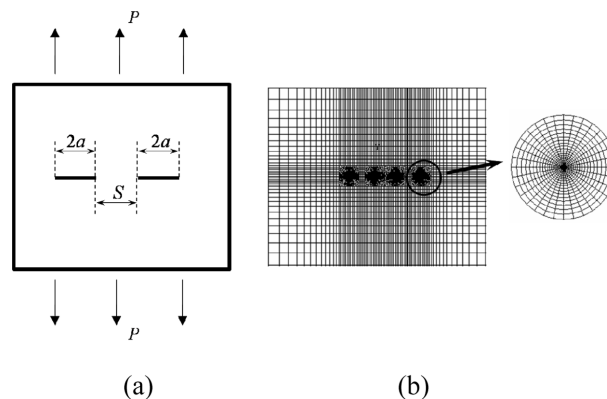


Fig. 1 Geometry (a) and finite element model (b) of two collinear cracks

calculation convergence at the crack-tip region, a sufficiently fine mesh as shown in Fig. 1(b) was used in the crack-tip region; the ratio of the finest element size around the crack-tip field to the crack length is reduced to 0.002. In addition, the 1/4 node elements were introduced at the crack tip to resolve singularity of the stress field. With increasing the distance from the crack tip, the grid gets coarser.

In all calculations, as shown in Fig. 1(a), a constant mechanical load, which was kept at 100 MPa if without declaration, was applied to the model in the small-scale and extensive creep stages. The $C(t)$ -integral, which obtained from the value of four contour was extracted from the built-in procedures of the software ABAQUS for comparison with the values determined from the Riedel and Rice's short estimation formula (Riedel and Rice 1980), and the Ehlers and Riedel's approximate interpolation formula (Ehlers and Riedel 1981). The constraint A_2 in the higher-order asymptotic $C(t) - A_2(t)$ solution was determined by using the point matching technique (Chao *et al.* 2001).

4. Numerical results and discussion

Prior to show calculation results of the two collinear cracks, the $C(t)$ -integral for a single crack along different paths was determined. Time-dependent variations of four different $C(t)$ -integral contours at the crack tip were shown in Fig. 2. With the increase of time, the $C(t)$ -integral contour decreases exponentially at $t < 10$ h and is then parabolically reduced at $t < 20$ h, which is in the coverage of the small-scale creep stage. With further increase of time, no distinct variation of the contour $C(t)$ -integral can be detected for all curves, which gradually approach to the constant value 0.0011 N/mm·h at $t > 80$ h. Hereafter, the time $t_T = 90$ h is defined as the transition time between the small-scale and extensive creeping stages in the following computations, which is in favorable agreement with the approximate calculation $t_T = K_I^2 \cdot (1 - \nu^2) / (n + 1) \cdot E \cdot C^*$ by Li *et al.* (2007).

To precisely determine the parameter $C(t)$ -integral for subsequent analysis of two collinear cracks, variations of the $C(t)$ -integral contours in the small-scale and extensive creep stages were calculated by using the finite element analysis and two empirical $C(t)$ -integral definitions, e.g., the Riedel and Rice's short estimation formula (Riedel and Rice 1980) and the Ehlers and Riedel's approximate

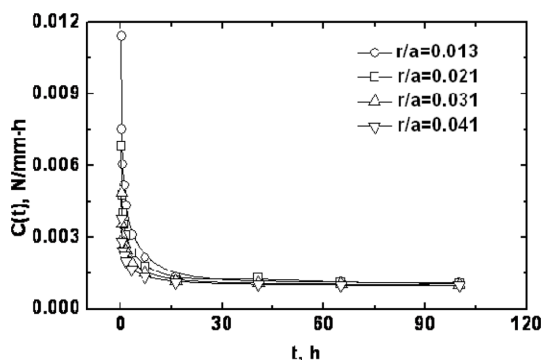


Fig. 2 Evaluation of $C(t)$ -integral along different paths for single crack model

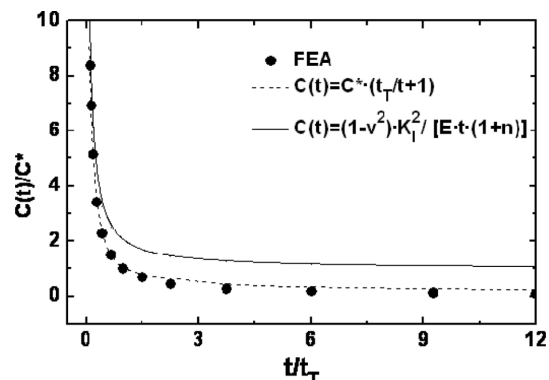


Fig. 3 Variation of $C(t)$ -integral with time for single crack model

interpolation formula (Ehlers and Riedel 1981). As shown in Fig. 3, the $C(t)$ -integral determined by the finite element analysis decreases rapidly at $t/t_T < 1$ and is then slowly reduced to a constant value with the increase of the creeping time. A comparative view shows that the calculation results by the Riedel and Rice's short estimation formula match well with that of the finite element analysis, while large deviation was found for the results by the Ehlers and Riedel's approximate interpolation formula. Accordingly, the $C(t)$ -integral is determined from the Riedel and Rice's short estimation formula in the following computations by using the higher-order asymptotic $C(t) - A_2(t)$ approach.

Fig. 4 displayed variation of the time-dependent constraint $A_2(t)$ in the higher-order asymptotic solution along different paths ($r/a = 0.013, 0.041, 0.102$) in the single crack model. As indicated in Fig. 4, at the small-scale creep stage $t/t_T < 0.5$, the constraint $A_2(t)$ increases rapidly with the increase of the creeping time for all paths around the crack tip; with increasing creep time from $t/t_T = 1$ up to 5, no discernible variation of the constraint $A_2(t)$ is detected, which is almost kept constant to $-0.96, -1.04, -1.1$ for the paths $r/a = 0.013, 0.041,$ and 0.102 , respectively. This confirms the fact that the constraint $A_2(t)$ in the three-term asymptotic solution of the power-law creeping material (Chao *et al.* 2001) is approximately independent of the creeping time at the extensive creep stage. Accordingly, if without special declaration, the constraint $A_2(t)$ in computation is hereafter denoted as the time independent constraint A_2^* at the extensive creep stage. In the majority of the subsequent discussion, the main concern would be placed on the stress state of the crack tip at $t/t_T = 1$.

Detailed information regarding spatial variation of the constraint A_2 at the creeping time $t/t_T = 1$ for the single crack model is displayed in Fig. 5. As shown in Fig. 5, with increasing distance from the crack tip, the constraint A_2 increases, and then the value of the constraint A_2 approaches to a constant as the distance far away from the crack tip, so the constraint A_2 is independent on the position ahead of the crack tip as the distance far away from the crack tip, and the constant value of the constraint A_2 is defined as the level of the constraint at this condition.

To see the significance of the crack-tip constraint analysis, a comparative view of the calculation results determined from the HRR-type field and higher-order asymptotic $C(t) - A_2(t)$ solution were supplied in reference to that from the finite element analysis. Fig. 6 shows the distributions of $\sigma_{\theta\theta}/\sigma_0$ in the crack tip region for the collinear crack models $S/a = \infty$ (single crack), 0.8 and 0.4 at the creeping time $t/t_T = 0.4, 1$ and 10. It is obvious that the results of the higher-order asymptotic $C(t) -$

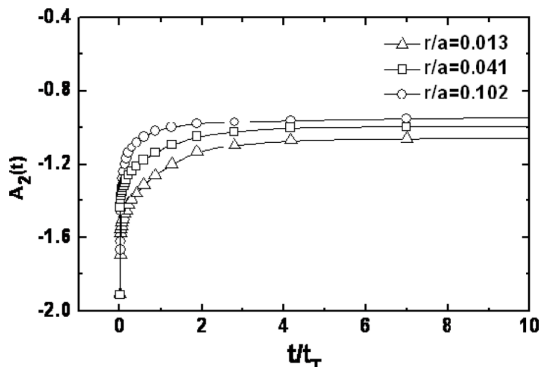


Fig. 4 Variation of constraint $A_2^*(t)$ with time along different paths for single crack model

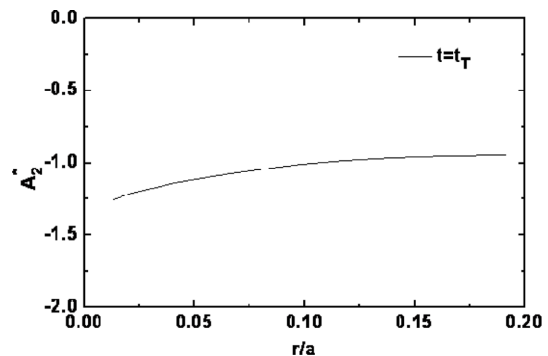


Fig. 5 Variation of constraint A_2^* at crack tip for single crack model

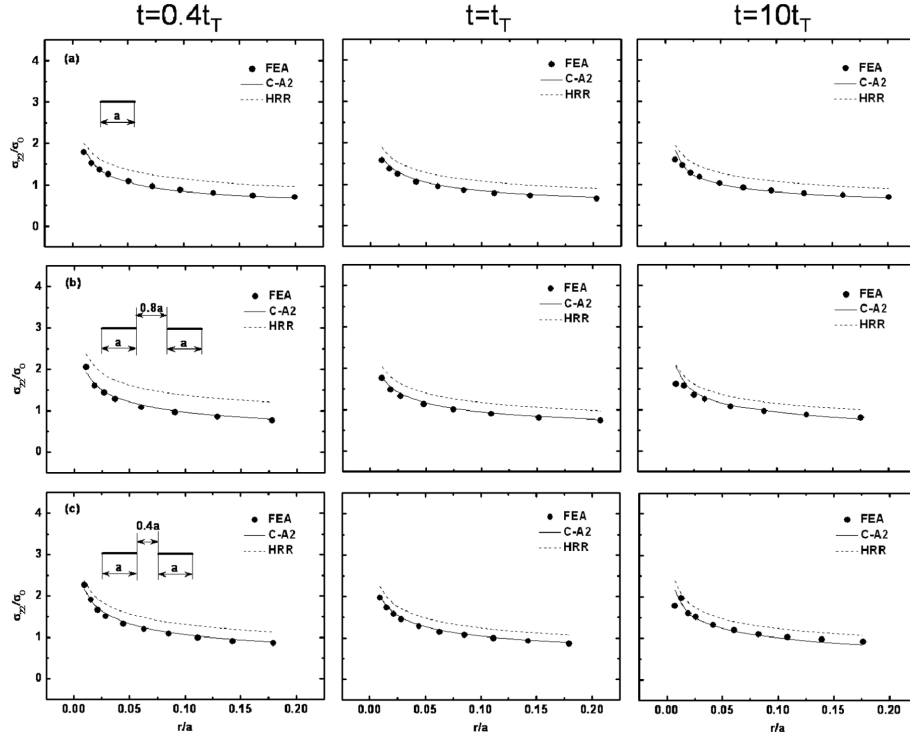


Fig. 6 Variation of $\sigma_{\theta\theta}/\sigma_0$ with distance from the crack tip at different creep time ($t = 0.4t_T$, $t = t_T$, $t = 10t_T$) (a) single crack model, (b) collinear crack model with $S/a = 0.8$, (c) collinear crack model with $S/a = 0.4$

$A_2(t)$ solution are in favorable agreement with that of the finite element analysis for the crack tip region up to $r/a < 0.20$, while the calculation of the HRR-type field results is in a significant deviation for all configurations. For the single crack model as shown in Fig. 6(a), the difference

between results of the HRR-type field and the higher-order asymptotic $C(t) - A_2(t)$ solutions slightly decrease with increase of the creeping time. Moreover, the event of stress relaxation at the crack-tip field with increase of the creeping time is observed. For the collinear crack model with the distance $S/a = 0.8$ as shown in Fig. 6(b), similar tendency of crack-tip $\sigma_{\theta\theta}/\sigma_0$ in response to the creeping time is found. However, for the collinear crack model with the distance $S/a = 0.4$ as shown in Fig. 6(c), under the condition of creeping time $t/t_T = 0.4$, the value of $\sigma_{\theta\theta}/\sigma_0$ at the crack-tip field is small compared with that obtained from the single crack model and the collinear crack model with distance $S/a = 0.8$. And the creeping time has little influence on the value of $\sigma_{\theta\theta}/\sigma_0$ at the crack-tip field.

Now we turn to influence of the mechanical load on the crack-tip constraint analysis of two collinear cracks under creep condition. Distributions of crack-tip $\sigma_{\theta\theta}/\sigma_0$ with different mechanical loads ($P = 100$ MPa, 200 MPa and 300 MPa) were plotted in Fig. 7. A global view of all cases in Fig. 7 shows that the calculations by using the higher-order asymptotic $C(t) - A_2(t)$ solution result in a good prediction of the crack-tip stress state, which agrees well with the finite element analysis. For the single crack model as shown in Fig. 7(a), the difference between results of the HRR-type field and the higher-order asymptotic $C(t) - A_2(t)$ solutions increases with increasing the mechanical loads, indicating the decreasing constraint. It is similar to the results of the collinear crack model

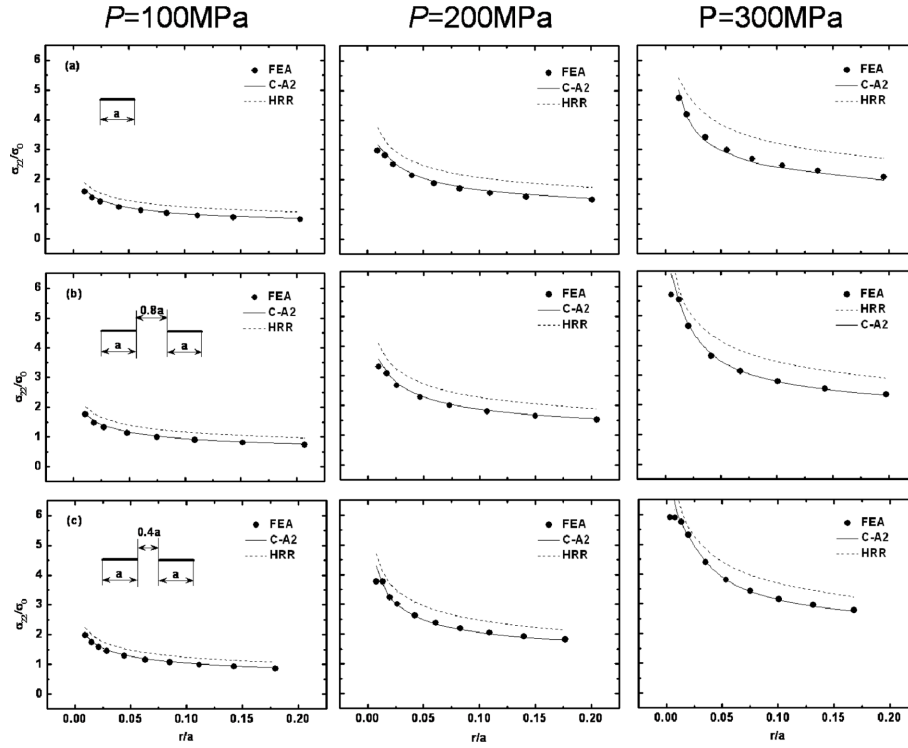


Fig. 7 Variation of $\sigma_{\theta\theta}/\sigma_0$ with distance from the crack tip at different mechanical loads ($P = 100\text{ MPa}$, 200 MPa , 300 MPa) (a) single crack model, (b) collinear crack model with $S/a = 0.8$, (c) collinear crack model with $S/a = 0.4$

with the distance $S/a = 0.8$, as shown in Fig. 7(b), the difference between results of the above-mentioned two methods increases with increasing the mechanical load. For the collinear crack model with the distance $S/a = 0.4$, similar tendency of crack-tip $\sigma_{\theta\theta}/\sigma_0$ in response to the mechanical load can also be found as shown in Fig. 7(c).

This gives a hint of the decreasing constraint for both of the single crack model and the collinear crack model with increasing the mechanical load.

5. Conclusions

In the present study, the higher-order asymptotic $C(t) - A_2(t)$ solution was introduced to investigate the crack-tip stress state of two collinear cracks, which occur in a power-law creeping material under the plane strain conditions. The results by using the HRR-type field and the finite element analysis were provided to check the constraint significance and the calculation accuracy of the higher-order asymptotic $C(t) - A_2(t)$ solution, respectively. A favorable agreement of the time-dependent contour integral $C(t)$ between the results obtained from the present finite element analysis and the Ehlers and Riedel's approximate interpolation formula was determined. The influence of the horizontal distances between two cracks on the constraint A_2 at the crack-tip field was analyzed. In comparison with the HRR-type field, the stress component $\sigma_{\theta\theta}$ obtained from the higher-order

asymptotic $C(t) - A_2(t)$ solution agreed well with that of the finite element analysis. The calculations shows that no discernible difference of the constraint A_2 was found at $t/t_T \geq 1$, and the creep time and the mechanical loads have no distinct influence on accuracy of the results obtained from the higher-order asymptotic $C(t) - A_2(t)$ solution.

Acknowledgments

This work was supported by national Natural Science Foundation of China ((No. 50906049)) and Research Project of State Key Laboratory of Mechanical System and Vibration (No. MSV201115).

References

- Assire, A., Michel, B. and Raous, M. (2001), "Creep crack initiation and creep crack growth assessments in welded structures", *Nucl. Eng. Des.*, **206**, 45-46.
- ASME (2004), *Boiler and Pressure Vessel Code Section XI*, New York, USA.
- Bassani, J.L. and McClintock, F.A. (1981), "Creep relaxation of stress around a crack tip", *Int. J. Solid Struct.*, **17**, 479-492.
- Betegon, C. and Hancock, J.W. (1991), "Two parameter characterization of elastic-plastic crack-tip fields", *J. Appl. Mech.*, **58**, 104-110.
- BS7910 (2005), *Guidance on Methods of Assessing the Acceptability of Flaws in Metallic Structure*, British Standard Institution, London.
- Bettinson, A.D., O'Dowd, N.P., Nikbin, K.M. and Webster, G.A. (2002), "Experimental investigation of constraint effects on creep crack growth", *ASME PVP*, **434**, 143-150.
- Budden, P.J. and Dean, D.W. (2007), "Constraint effects on creep crack growth", *Proceedings of the 8th International Conference Creep and Fatigue at Elevated Temperatures*, San Antonio, Texas, July.
- Chao, Y.J., Zhu, X.K. and Zhang, L. (2001), "Higher-order asymptotic crack-tip fields in a power-law creeping material", *Int. J. Solids Struct.*, **38**, 3853-3875.
- Chao, Y.J. and Zhu, X.K. (1998), "J-A2 Characterization of crack-tip fields: Extent of J-A2 dominance and size requirements", *Int. J. Fract.*, **89**, 285-307.
- Chen, Y.Z., Wang, Z.X. and Lin, X.Y. (2009), "Evaluation of the T-stress for interacting cracks", *Comput. Mater. Sci.*, **45**(2), 349-357.
- Ehlers, R. and Riedel, H. (1981), "A finite element analysis of creep deformation in specimen containing a macroscopic crack", *Advances in Fracture Research, Proceeding of The Fifth International Conference on Fracture*, Cannes, France, June.
- Fookes, A.J. and Smith, D.J. (2003), "The influence of plasticity in creep crack growth in steels", *Int. J. Press. Vessel. Pip.*, **80**, 453-463.
- Hutchinson, J.W. (1968), "Singular behavior at the end of a tension crack in a hardening material", *J. Mech. Phys. Solids*, **16**, 13-31.
- Kamaya, M. (2008), "Growth evaluation of multiple interacting surface cracks. PartI: Experiments and simulation of coalesced crack", *Eng. Fract. Mech.*, **75**(6), 1136-1349.
- Kamaya, M. (2008), "Growth evaluation of multiple interacting surface cracks. PartII: Growth evaluation of parallel cracks", *Eng. Fract. Mech.*, **75**(6), 1350-1366.
- Kim, Y.J., Kim, J.S. and Huh, N.S. (2002), "Engineering C-integral estimates for generalized creep behavior and finite element validation", *Int. J. Press. Vessel. Pip.*, **79**, 427-443.
- Li, F.Z., Needleman, A. and Shih, C.F. (1988), "Characterization of near tip stress and deformation fields in creeping solid", *Int. J. Fract.*, **36**, 163-186.
- Liu, X., Xuan, F.Z., Si, J. and Tu, S.D. (2008), "Expert system for remaining life prediction of defected components under fatigue and creep-fatigue loading", *Expert Syst. Appl.*, **34**, 222-230.

- O'Dowd, N.P. and Shih, C.F. (1991), "Family of crack-tip fields characterized by a triaxiality parameter-I: structure of fields", *J. Mech. Phys. Solids*, **39**, 989-1015.
- R6 (2006), *Assessment of the Integrity of Structures Containing Defects, Revision 4*, British Energy Generation Ltd, Gloucester.
- Rice, J.R. and Rosengren, G.F. (1968), "Plane strain deformation near a crack tip in a power-law hardening material", *J. Mech. Phys. Solids*, **16**, 1-12.
- Riedel, H. and Rice, J.R. (1980), "Tensile cracks in creeping solids", *Fracture Mechanics: Twelfth Conference, ASTM STP700, American Society for Testing and Materials*, 112-130.
- Sharma, S.M., Aravas, N. and Zelman, M.C. (1995), "Two-parameter characterization of crack-tip fields in edge-cracked geometries: Plasticity and Creep Solution", *Fract. Mech.*, **25**, 309-327.
- Shih, C.F., O'Dowd, N.P. and Kirk, M.T. (1993), "A framework for quantifying crack-tip constraint. Constraint effect in fracture", *ASTM STP 1171, American Society for Testing and Materials*, Philadelphia.
- Si, J., Xuan, F.Z. and Tu, S.T. (2008), "A numerical creep analysis on the interaction of twin semi-elliptical cracks", *Int. J. Press. Vessel. Pip.*, **85**, 459-467.
- Sun, P.J., Wang, G.Z., Xuan, F.Z., Tu, S.T. and Wang, Z.D. (2011), "Quantitative characterization of creep constraint induced by crack depths in compact tension specimens", *Eng. Fract. Mech.*, **78**, 653-665.
- Wang, G.Z., Liu, X.L., Xuan, F.Z. and Tu, S.T. (2010), "Effect of constraint induced by crack depth on creep crack-tip stress field in CT specimens", *Int. J. Solids Struct.*, **47**, 51-57.
- Wang, G.Z., Li, B.K., Xuan, F.Z. and Tu, S.T. (2012), "Numerical investigation on the creep crack-tip constraint induced by loading configuration of specimens", *Eng. Fract. Mech.*, **79**, 353-362.
- Xuan, F.Z., Si, J. and Tu, S.T. (2009), "Evaluation of C^* integral for interacting cracks in plates under tension", *Eng. Fract. Mech.*, **76**, 2192-2201.
- Yang, L., Sutton, M.A., Deng, X. and Lyons, J.S. (1996), "Finite element analysis of creep fracture initiation in a model super-alloy material", *Int. J. Fract.*, **81**, 299-320.
- Yang, S., Chao, Y.J. and Sutton, M.A. (1993), "Higher order asymptotic fields in a power law hardening material", *Eng. Fract. Mech.*, **45**, 1-20.
- 579-1/ASME FFS-1 (2007), *Fitness-for-service*, Section 9., American Society of Mechanical Engineers.